sciendo Radiology and Oncology | Ljubljana | Slovenia | www.radioloncol.com RADIOLOGY AND ONCOLOGY

research article

Breast size and dose to cardiac substructures in adjuvant three-dimensional conformal radiotherapy compared to tangential intensity modulated radiotherapy

Ivica Ratosa[1,2], Aljasa Jenko[1], Zeljko Sljivic[1,3], Maja Pirnat[4], Irena Oblak[1,2]

[1] Department of Radiotherapy, Institute of Oncology Ljubljana, Ljubljana, Slovenia
[2] Faculty of Medicine, University of Ljubljana, Ljubljana, Slovenia
[3] Faculty of Health Sciences, University of Ljubljana, Ljubljana, Slovenia
[4] Department of Radiology, University Medical Centre Maribor, Maribor, Slovenia

Radiol Oncol 2020; 54(4): 470-479.

Received 18 March 2020
Accepted 10 May 2020

Correspondence to: Assist. Ivica Ratoša, M.D., Ph.D., Institute of Oncology Ljubljana, Zaloška cesta 2, SI-1000 Ljubljana, Slovenia.
E-mail: iratosa@onko-i.si

Disclosure: No potential conflicts of interest were disclosed.

Background. The aim of the study was to quantify planned doses to the heart and specific cardiac substructures in free-breathing adjuvant three-dimensional radiation therapy (3D-CRT) and tangential intensity modulated radiotherapy (t-IMRT) for left-sided node-negative breast cancer, and to assess the differences in planned doses to organs at risk according to patients' individual anatomy, including breast volume.

Patients and methods. In the study, the whole heart and cardiac substructures were delineated for 60 patients using cardiac atlas. For each patient, 3D-CRT and t-IMRT plans were generated. The prescribed dose was 42.72 Gy in 16 fractions. Patients were divided into groups with small, medium, and large clinical target volume (CTV). Calculated dose distributions were compared amongst the two techniques and the three different groups of CTV.

Results. Mean absorbed dose to the whole heart (MWHD) (1.9 *vs.* 2.1 Gy, $P < 0.005$), left anterior descending coronary artery mean dose (8.2 *vs.* 8.4 Gy, $P < 0.005$) and left ventricle (LV) mean dose (3.0 *vs.* 3.2, $P < 0.005$) were all significantly lower with 3D-CRT technique compared to t-IMRT. Apical (8.5 *vs.* 9.0, $P < 0.005$) and anterior LV walls (5.0 *vs.* 5.4 Gy, $P < 0.005$) received the highest mean dose (D_{mean}). MWHD and LV-D_{mean} increased with increasing CTV size regardless of the technique. Low MWHD values (< 2.5 Gy) were achieved in 44 (73.3%) and 41 (68.3%) patients for 3D-CRT and t-IMRT techniques, correspondingly.

Conclusions. Our study confirms a considerable range of the planned doses within the heart for adjuvant 3D-CRT or t-IMRT in node-negative breast cancer. We observed differences in heart dosimetric metrics between the three groups of CTV size, regardless of the radiotherapy planning technique.

Key words: breast cancer; breast size; 3D-CRT; IMRT; heart dose; left anterior descending coronary artery

Introduction

Cardiovascular diseases are becoming the most critical competing mortality risk in women with early breast cancer treated with present-day radiotherapy (RT).[1,2] The relative risk of radiation-induced heart failure increases with rising cardiac radiation exposure, typically reported as mean absorbed dose to the whole heart (MWHD).[3-5] MWHD values reflect local radiation therapy practices, and with the help of modern RT approaches, now ranging from 1.7–5.4 Gy[6-8] and 1.22–1.65 Gy[9], for mean and median values, respectively. However, even very low cardiac exposure does not eliminate the risk of radiotherapy-mediated cardiotoxicity, which has been demonstrated in recent studies.[3,5,10]

In many recent publications, authors favor the use of intensity modulated techniques over three-dimensional conformal radiotherapy (3D-CRT) in node negative breast cancer adjuvant RT, arguing for lower MWHD, decreased skin toxicity and more homogeneous dose distribution in the target volume.[11-13] Besides the RT technique used, MWHD depends on the position of the patient's heart relative to the irradiated breast and the shape of their chest wall.[14] Different simple anatomical measures were evaluated to predict increased MWHD and subsequently for the need to use one of the heart-sparing techniques, namely deep inspiration breath hold technique (DIBH). Useful anatomical measures are increased chest wall separation (CWS)[9], maximum heart distance (the distance between the anterior cardiac contour crossing over the posterior edge of the tangential fields)[15], multidimensional assessment of the presence of the heart in contact with the chest wall[14] and linear heart contact distance from the left sternal to the beginning of the lung parenchyma edges at the 4th costal arch in the axial axis.[16] It has also been shown that the shape and size of the clinical target volume (CTV) result in increased mean and/or maximum point heart doses.[9,17,18] If a cohort of breast cancer patients with similar breast volume is defined, specific problems and resolutions can be proposed, because breast contours according to breast size and shape may be associated with the variations in the target volume coverage and calculated dose to organs at risk.[19] Three-dimensional treatment planning allows target volume to be measured and CTVs of ≤ 500–975 cm^3, 975–1.600 cm^3 and ≥ 1.600 cm^3 have been typically, but not consistently, defined as small, medium and large breasts, respectively.[20,21] Additionally, quite a few clinical studies have reported a comparison of the clinical adverse events in regard to the three groups of breast sizes.[22]

Although observed average MWHD in a population of breast cancer survivors is low, smaller fragments of the heart might have received doses exceeding 25–40 Gy.[4,10,23,24] Subclinical cardiac dysfunction was observed early after adjuvant radiotherapy for breast cancer with molecular biomarkers[25,26], radionuclide myocardial perfusion imaging[27–29], echocardiography[30–32], and functional magnetic resonance imaging.[31] Limited data exist regarding the range of doses received by individual heart substructures with adjuvant free-breathing 3D-CRT or tangential intensity modulated radiotherapy (t-IMRT) for left-sided breast cancer. It has been shown that MWHD does not necessarily correlate to mean radiation doses, absorbed by cardiac chambers or coronary arteries in adjuvant breast cancer radiotherapy.[33–36] Lately, detailed studies of the specific cardiac structures' absorbed radiation dose in thoracic radiation therapy[24,36,37], and the efforts to understand the specific radiation dose-volume effects in the heart have emerged. [4,38–41] With expanding knowledge in this field, German Society of Radiation Oncology (DEGRO) recommends new stringent dose constraints for the heart and its substructures: MWHD < 2.5 Gy, left ventricle (LV) D_{mean} < 3 Gy (LV mean dose), LV V_5 < 17% (volume of LV receiving ≤ 5 Gy), LV V_{23} < 5% (volume of LV receiving ≤ 23 Gy), left anterior descending coronary (LADCA) D_{mean} < 10 Gy (LADCA mean dose), LADCA V_{30} < 2% (volume of LADCA receiving ≤ 30 Gy), and LADCA V_{40} < 1% (volume of LADCA receiving ≤ 40 Gy).[42]

To standardize the reporting of cardiac imaging regardless of diagnostic modality, both The American Society of Echocardiography and the European Association of Cardiovascular Imaging recommend using a segmentation model of the LV to assess regional LV function.[42,44] The LV segmentation model reflects coronary arteries' territories and permits to compare echocardiography with other imaging modalities.[43] Five main LV segments, defined in a cardiac atlas by Duane *et al*.[24] are based on a previously described 17-segmentation model.[44]

In this work, we hypothesized that in the setting of the node-negative left-sided breast cancer adjuvant radiotherapy, the lowest median MWHD and doses to the cardiac substructures would be achieved with the t-IMRT, compared to 3D-CRT. In addition, we assumed that individual patient characteristics, which include chest wall separation and breast volume, would contribute to the differences in absorbed doses to the heart and cardiac substructures, regardless of the treatment planning technique. To test our hypothesis, we aimed to quantify doses to the heart and cardiac substructures in present-day free-breathing adjuvant 3D-CRT and t-IMRT and to analyze the differences in dosimetric metrics to organs at risk between three different groups of CTV according to breast size and other individual anatomical information.

Patients and methods

Patient selection and CT simulation

The study was approved by the ethics review board committee (approval number KME 78/07/15). Based on the size of the CTV, we randomly selected

TABLE 1. Target goals used in the planning process

Structure	Target goals
PTV	D_2% < 108%
PTVeval	V_{95}% > 95%
Whole Body Contour	Global D_{max} < V110%
Heart	D_{mean} < 3.2 Gy V_{17} Gy < 10% V_{35} Gy < 5%
Ipsilateral Lung	D_{mean} < 10 Gy V_{17} Gy < 25% V_{26} Gy < 20%
Bilateral lung	D_{mean} < 3.2 Gy

D_{max} = maximum dose; D_{mean} = mean dose; Dx % = absorbed dose, received by x % of the PTV; PTV = planning target volume; PTVeval = planning target volume for evaluation; V_x% = fractional volume, receiving x % of the prescribed dose; V_x Gy = fractional volume receiving x Gy

patients with early left-sided node-negative breast cancer. The definitions of the small, medium, and large breast volumes were like those made available elsewhere.[22] The patients were referred to adjuvant radiotherapy between the years 2014 and 2015. All patients underwent a free-breathing non-enhanced simulation computed tomography (CT) scan with a 3 mm slice thickness. The treatment position for all women was supine, on an inclined simulation table using a breast board, with both arms positioned above the head.

Delineation, treatment planning, and data collection

Whole heart, LV with its anterior, apical, inferior, lateral, and septal walls, right ventricle (RV), left atrium (LA), right atrium (RA), LADCA with proximal, middle and distal segments, right coronary artery (RCA), left circumflex coronary artery (LCX), and left main coronary artery (LMCA) were delineated by one radiation oncologist. We followed identification of the individual structure segments by the instructions proposed by Duane *et al*.[24] in a recently published heart atlas. We used a 6 mm diameter for all coronary arteries' segments, as previously proposed.[23] The thickness of the LV wall was set to 10 mm. An experienced cardiac radiologist reviewed the contoured cardiac segments. We delineated CTV to include total glandular breast tissue according to published guidelines.[45] Planning target volume (PTV) was generated by adding a 5 mm uniform margin to the CTV, and the planning target volume for evaluation (PTVeval) was created similarly, with a modification that excludes 5 mm below the skin surface. Additionally, we collected anatomically based distance metrics, such as chest wall separation (CWS) and a previously described "4th arch" metric.[16]

We used Monaco (Elekta AB®, Stockholm, Sweden) as a contouring and treatment planning platform. The prescribed dose was 42.72 Gy in 16 fractions, 5 days per week. For the 3D-CRT treatment planning, we used 6MV photon tangential beam arrangement with wedge filters and additional 6MV or 15MV small beams in tangential or non-tangential beam direction where needed to achieve a homogeneous dose distribution. The "Collapsed Cone" algorithm was used to calculate the dose. For t-IMRT plans we used the same isocenter position as with 3D-CRT planning and two tangential 6 MV photon beams positioned in the same direction as for 3D-CRT plans. The plans were calculated using inverse dose optimization with "Monte-Carlo" algorithm. Dynamic Multileaf Collimator (dMLC) technique was used with minimum segment size 1 cm and 30 control points, which generated 25–30 segments per beam. Although "the dose-to-water" reporting is typically used in clinical routine for the inverse optimization treatment plans and since "Collapsed Cone" algorithm does not have that option for calculation, we used "the dose-to-medium" reporting in our study for both 3D-CRT and t-IMRT planning in order to improve treatment plan comparability.

In the planning optimization procedure, we used institutional target goals for both treatment plans (Table 1). Dose constraints for the specific cardiac substructures were not incorporated into the optimization process but we strived to keep the dose to the whole heart as low as possible without compromising the target coverage for both techniques. Each plan was thoroughly evaluated for target coverage and OAR. We reported nominal median absolute doses, without EQD_2 (equivalent dose in 2 Gy per fraction) conversion. All treatment plans were created by one dosimetrist and one medical physicist.

Statistical analyses

Calculated dose distributions were compared amongst the two techniques and the three different groups of CTV. Due to mostly non-parametrically distributed data, dose distributions data between the groups were compared using the Kruskal-Wallis and Mann-Whitney tests. Friedman ANOVA and Wilcoxon signed-rank test were also used to compare values between the two techniques. All

TABLE 2. Target volumes' and organs at risk's metrics

Target volume/ Organ at risk	The whole group N = 60	Small CTV N = 22	Medium CTV N = 21	Large CTV N = 17	p value
CTV [cm^3]	800.6 (124.8–2970.9)	425.7 (124.8–545.5)	867.0 (652.1–1295.1)	1586.8 (1348.9–2970.9)	0.021
PTVeval [cm^3]	990.7 (233.5–3336.1)	583.0 (233.5–711.1)	1035.9 (834.3–1576.5)	1874.3 (1605.8–3336.1)	< 0.005
PTV [cm^3]	1163.3 (340.1–3792.2)	730.7 (340.1–856.6)	1212.3 (985.1–1805)	2134.8 (1826.4–3792.2)	< 0.005
CWS [cm]	23.1 (17.9–33.2)	19.5 (17.9–23.2)	24.0 (19.9–28.5)	27.5 (22.9–33.2)	< 0.005
4th arch metrics [cm]	4.4 (0–11.6)	1.6 (0–9.6)	5.5 (0–11.6)	7.1 (0–10.7)	0.008
Heart [cm^3]	677.7 (432.9–1192.7)	625.2 (432.9–912.8)	671.1 (563.5–872.4)	817.9 (620.1–1192.7)	< 0.005
Left Ventricle [cm^3]	173.8 (116–277.4)	161.3 (116–251.7)	173.8 (120.8–229.8)	188.7 (147.4–277.4)	0.018
Left Lung [cm^3]	1245.1 (809.3–2127.9)	1458.9 (824.5–2127.9)	1123.8 (944.2–1619.2)	1230.6 (809.3–1541.7)	0.003
Right Lung [cm^3]	1563.4 (855–2560.1)	1721.9 (992.9–2560.1)	1466.4 (855.1–1838.2)	1493.2 (1089.6–1925.6)	0.002
Lungs [cm^3]	2879.7 (1504.6–4789.2)	3241.3 (1877.5–4789.2)	2634.4 (1504.6–3513.6)	2799.8 (1960.2–3479.2)	0.001

CTV = clinical target volume; CWS = chest wall separation distance at isocenter; PTV = planning target volume; PTVeval = planning target volume for evaluation

numbers are presented as median values with a range. Statistical analyses were performed with IBM® SPSS® version 24.0 (SPSS Inc., Armonk: NY, IBM corporation). We considered a p-value ≤ 0.05 as statistically significant.

Results

Patient population and treatment plans

Sixty patients with left-sided breast cancer were included in this analysis, divided into groups of small (N = 22, 36.6%), medium (N = 21, 35.0%) and large (N = 17, 28.4%) CTV size. Target volumes' and OAR's metrics are presented in Table 2.

There was a statistically significant difference between the three groups for all measured target volumes, OAR volumes, and anatomically based simple distance metrics. Regarding target coverage, all except two dosimetric parameters (PTVeval V_{107}%, PTVeval D_2%), were superior in the 3D-CRT group (Tables 3 and 4). Nevertheless, the t-IMRT approach resulted in lower high-dose areas (PTVeval V_{105}%) across all three CTV groups.

Whole heart

For the whole group of evaluated patients, 3D-CRT technique showed significant lower MWHD compared to t-IMRT (Table 5) with an absolute difference of 0.2 Gy.

Absolute difference in MWHD between the two techniques ranged from 0.06, 0.46 and 0.7 for the groups of medium-, large- and small-sized CTVs, respectively (Table 6). CTV size had an impact on MWHD regardless of the RT technique, while other parameters were not statistically different except for heart-V_5 Gy in 3D-CRT technique. In 3D-CRT, MWHD correlated with increased CWS relative to 18.0 cm (0.09 Gy/1 cm, p = 0.0022) and with CTV size (0.06 Gy/100 cm^3, p = 0.0015). Low MWHD values (< 2.5 Gy) were achieved in 44 (73.3%) and 41 (68.3%) patients for 3D-CRT and t-IMRT techniques, correspondingly (Figure 1).

Heart chambers

Selected dose-volume parameters for the LV are presented in Table 5 and 6. For the whole group, 3D-CRT showed lower dosimetric metrics for the

TABLE 3. Target volume dosimetric metrics

Target volume	3D-CRT	t-IMRT	p value
PTVeval D_{98}% [Gy]	40.6 (39.8–41.4)	40.3 (38.7–41.6)	0.002
PTVeval D_2% [Gy]	44.7 (44.4–45.5)	43.8 (43.8–47.1)	NS
PTVeval D_{50}% [Gy]	43.3 (42.7–43.7)	42.9 (42.2–43.9)	< 0.005
PTVeval V_{95}% [%]	98.1 (95.3–99.6)	96.8 (79.9–99.9)	0.001
PTVeval V_{105}% [%]	1.3 (0.1–10.3)	4.3 (0.01–85.9)	< 0.005
PTVeval V_{105}% [cm^3]	11.7 (0.08–656.7)	5.4 (0.06–68.0)	0.014
PTVeval V_{107}% [%]	0 (0–1.4)	0.1 (0–9.6)	< 0.005
PTVeval V_{107}% [cm^3]	0 (0–321.4)	0 (0–7.2)	NS
PTVeval V_{110}% [%]	0 (0–0)	0 (0–0)	NS
D_{max} [Gy]	45.7 (45.1–46.9)	46.9 (45.3–51)	< 0.005

3D-CRT = three-dimensional conformal radiotherapy; D_2% = near maximum dose, D_{50}% = median dose; D_{98}% = near minumum dose, D_{max} = maximal absorbed dose, NS = not significant; PTVeval = planning target volume for evaluation; t-IMRT = tangential intensity modulated radiation therapy; V_x% = fractional volume, receiving x % of the prescribed dose

TABLE 4. Target volume dosimetric metrics and CTV size

Target volume	Small CTV	Medium CTV	Large CTV	p value (S vs. M vs. L)
3D-CRT PTVeval V_{95}% [%]	97.7 (95.3–99.6)	98.3 (96.2–99.5)	98.8 (97.5–99.4)	0.022 (S vs. M, S vs. L)
t-IMRT PTVeval V_{95}% [%]	97.9 (96.3–99.2)	97.3 (95.3–99.0)	96.8 (79.9–99.9)	NS
p value (3D-CRT *vs.* T-IMRT)	NS	p = 0.003	p = 0.013	
3D-CRT PTVeval V_{105}% [cm^3]	8.1 (0.5–17.5)	12.5 (0.08–91.3)	87.3 (9.5–656.6)	< 0.005 (S vs. M, S vs. L, M vs. L)
t-IMRT PTVeval V_{105}% [cm^3]	7.4 (0.1–61.5)	5.9 (0.09–54)	4.2 (0.06–68.2)	NS
p value (3D-CRT *vs.* T-IMRT)	NS	NS	p = 0.012	

3D-CRT = three-dimensional conformal radiotherapy; L = large; M = medium; NS = not significant; PTVeval = planning target volume for evaluation; S = small; t-IMRT = tangential intensity modulated radiation therapy; V_x% = fractional volume, receiving x % of the prescribed dose

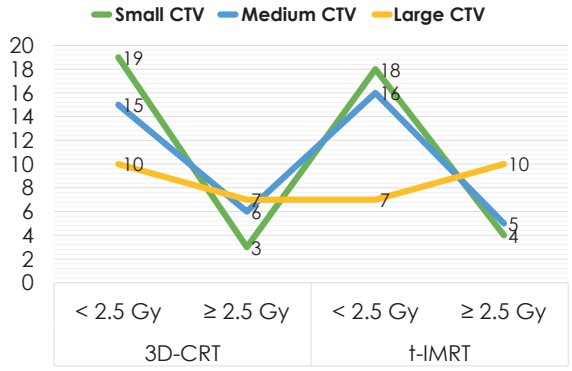

FIGURE 1. Mean whole heart dose and number of plans within each CTV groups, concerning optimal mean dose value.

3D-CRT = three-dimensional conformal radiotherapy; CTV = clinical target volume; Gy = Gray; t-IMRT = tangential intensity modulated radiation therapy

TABLE 5. Radiotherapy technique and selected dose-volume parameters for the whole heart and selected cardiac substructures

Parameter	3D-CRT	t-IMRT	p value*
MWHD [Gy]	1.90 (0.61–4.14)	2.13 (1.06–4.4)	< 0.005
LV-D_{mean} [Gy]	2.98 (0.78–8.03)	3.22 (1.31–7.25)	< 0.005
LV-V_5 Gy [%]	8.67 (0–26.3)	9.21 (0–26.02)	0.455
LV-V_{23} Gy [%]	2.46 (0–14.32)	1.86 (0–10.58)	0.003
LV anterior-D_{mean} [Gy]	5.00 (1.27–20.17)	5.42 (1.94–19.18)	< 0.005
LV apical-D_{mean} [Gy]	8.97 (1.22–24.89)	8.47 (1.64–22.16)	< 0.005
LADCA-D_{mean} [Gy]	8.20 (1.23–27.92)	8.39 (1.8–27.62)	< 0.005
LADCA-V_{30} Gy [%]	5.39 (0–66.34)	2.01 (0–84.20)	< 0.005
LADCA-V_{40} Gy [%]	0 (0–37.8)	0 (0–43.09)	< 0.005
LADCA-prox-D_{mean} [Gy]	2.17 (0.62–8.68)	2.66 (1.22–12.43)	< 0.005
LADCA-mid-D_{mean} [Gy]	9.63 (1.67–40.07)	11.05 (2.26–39.63)	0.956
LADCA-dist-D_{mean} [Gy]	13.73 (1.44–41.11)	15.93 (2.03–3.89)	0.132

*Wilcoxon signed-rank test; 3D-CRT = three-dimensional conformal radiotherapy; dist = distal; D_{mean} = mean dose; Gy = Gray; LADCA = left anterior descending artery; LV = left ventricle; mid = middle; MWHD = whole heart mean dose; prox = proximal; t-IMRT = tangential intensity modulated radiation therapy; V_x Gy = fractional volume receiving x Gy

LV contour, except for LV apical-D_{mean} and LV-V_{23} Gy. The lowest D_{mean} values of the dosimetric metrics for LV, including anterior, lateral, septal, and inferior LV wall, were obtained in the small CTV group, regardless of treatment technique.

In 3D-CRT, apical and anterior LV walls received the highest D_{mean} (Table 5), while lateral, septal, and inferior regions, received 1.9, 1.6, and only 0.6 Gy, respectively. The D_{mean} of RV, RA, and LA were 1.41 Gy (range, 0.5–4.8), 0.5 Gy (0.3–1.2), and 0.6 Gy (0.4–1.5), respectively and were not statistically significantly different among different groups of the CTV size. Likewise, with IMRT, apical and anterior LV walls received similarly high mean radiation doses. The D_{mean} varied from 8.5 Gy (range, 1.64–22.16), 5.4 Gy (1.94–19.18), 2.33 Gy (1.18–7.59), 2.18 Gy (1.01–4.46), and 1.11 Gy (0.77–1.98) for apical, anterior, lateral, septal and inferior LV walls, correspondingly. Seventeen-segmental LV models, represented as a Bull's eye diagram, with respective D_{mean} dose distributions, are presented in Figure 2. Low LV-D_{mean} (< 3 Gy), LV-V_5 (< 17%), and LV-V_{23} (< 5%) values were achieved in 51.6%, 88.3%, and 73.3% of treatment plans in 3D-CRT and in 41.6%, 88.3%, and 85.0% of treatment plans in t-IMRT, respectively.

Coronary arteries

Planned median D_{mean} values for LADCA and its segments are presented in Table 5. Median mean doses to other coronary arteries, namely RCA, LCX, and LMCA were 0.7 Gy (range, 0.3–4.7), 0.7 Gy (0.3–2.0), and 0.8 Gy (0.5–2.0), in the 3D-CRT group and 1.14 Gy (0.77–1.86), 1.10 Gy (0.79–2.18) and 1.31 Gy (0.96–2.17) in the t-IMRT group, respectively. For the entire group, only parameter LADCA-V_{30} Gy was found to be lower with t-IMRT compared to 3D-CRT technique, but the reduction

was seen only in the medium and large CTV-size groups.

Compared to t-IMRT, 3D-CRT technique showed advantages in terms of lower planned D_{mean} values of proximal, middle and distal LADCA segments (Table 5). However, dose to the proximal LADCA segment increased with the CTV size, regardless of the planning method. The highest D_{mean} values of the middle and distal LADCA segments were achieved in patients with the medium or large target volumes.

Low LADCA-D_{mean} (< 10 Gy), LADCA-V_{30} Gy (< 2%), and LADCA-V_{30} Gy (< 1%) values were achieved in 55.0%, 48.3%, and 71.6% of treatment plans in 3D-CRT and in 56.6%, 51.6%, and 86.6% of treatment plans in t-IMRT, respectively. Figure 2 represents Bull's eye diagrams of the LV and segment models of the coronary arteries with reported median D_{mean} distributions for 3D-CRT technique.

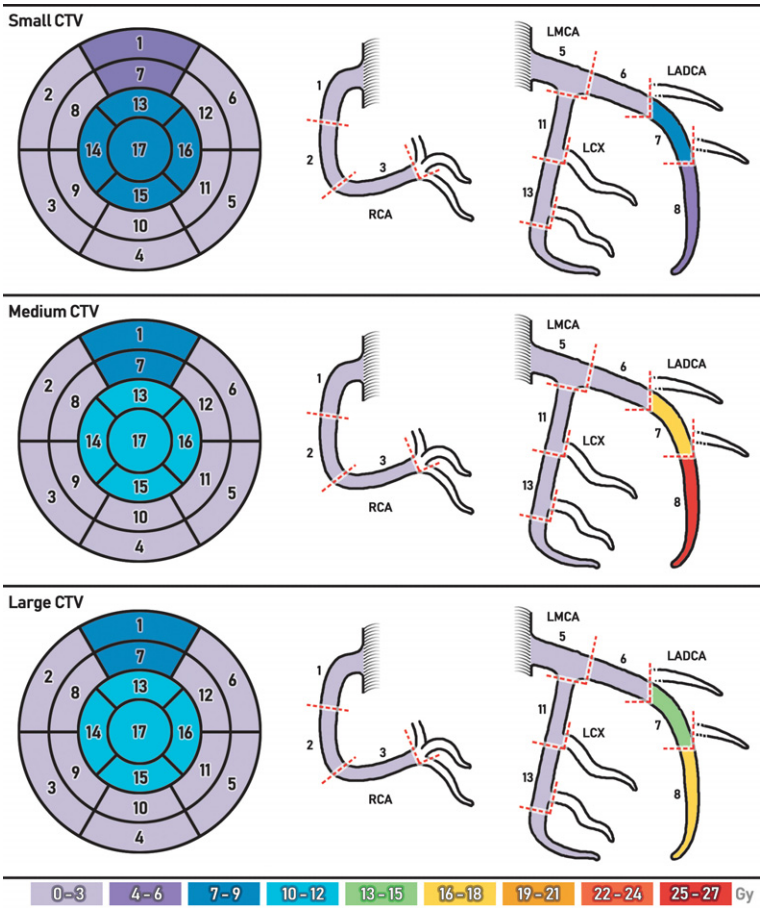

FIGURE 2. Bull's eye diagrams of the left ventricle and segment models of the coronary arteries with reported median D_{mean} distributions in three-dimensional conformal radiotherapy plans, divided in groups according to clinical target volume size. Contouring segments of left ventricle consisted of anterior (segments 1 and 7), apical (segments 13–17), inferior (segments 4 and 10), lateral (segments 5, 6, 11, 12) and septal regions (segments 2, 3, 8, 9).

CTV = clinical target volume; Gy = Gray; LADCA = left anterior descending artery; LCX = left circumflex artery; LMCA = left main coronary artery; RCA = right coronary artery

Discussion

By tradition and its contouring pragmatism, MWHD is the most frequently reported surrogate for the assessment of the potential subsequent cardiotoxic effects after radiation therapy for breast cancer. In the present study, we aimed to compare doses to the individual cardiac structures in the circumstances that represent everyday practice in free-breathing node-negative left-sided breast cancer adjuvant 3D-CRT or t-IMRT. Herein, we report reasonably low median MWHD values achieved with both techniques, 1.9 Gy with 3D-CRT and 2.1 Gy with t-IMRT. In the contemporary series, measured mean or median MWHD values in free-breathing node-negative left-sided breast cancer adjuvant RT are in the range of 2.6–3.6 Gy for 3D-CRT[6,33,35,36] and 1.8–4.8 for the intensity modulated techniques.[11,46,47]

In both evaluated techniques, we observed statistically significant differences between the groups of small, medium, and large CTV sizes for the following dose-volume parameters: MWHD, mean doses for proximal LADCA segment, anterior, lateral, inferior, and septal LV walls. In medium and large-sized CTV, we observed reduction of LADCA-D_{mean} with t-IMRT technique, which was not statistically different. Our results are consistent with previously published studies showing increased CWS, relative to 22 cm, to be one of the predictors for a higher MWHD, in both normo- and hypofractionation.[9] Other studies have also demonstrated the correlation between the calculated heart dose and increasing breast size, especially when PTV exceeds 1500 cm^3.[17,18] Compared to small-sized CTV, MWHD increased with medium- and large- sized CTVs in our study, although the absolute differences between the groups were relatively small, ranging from 0.73 Gy and 0.97 Gy for the t-IMRT and 3D-CRT, respectively. Our results imply that patients' anatomy, including CWS and/or CTV/PTV volume, should be also considered when choosing the appropriate radiotherapy technique (3D-CRT *vs.* modulated approaches), patient setup (prone or lateral *vs.* supine), and breathing adaptation techniques. As previously mentioned, breast size grouping could be useful in this context, helping to tailor whole breast irradiation.[19]

TABLE 6. Breast size and selected dose-volume parameters for the whole heart and cardiac substructures

Parameter	Small CTV		Medium CTV		Large CTV		p value
	3D-CRT	t-IMRT	3D-CRT	t-IMRT	3D-CRT	t-IMRT	
MWHD [Gy]	1.29 (0.61–3.75)	1.99 (1.06–3.98)	2.05 (1.06–3.84)	2.11 (1.62–3.54)	2.26 (1.04–4.14)	2.72 (1.46–4.4)	< 0.005*; 0.047†
Heart-V_5 Gy [%]	2.56 (0.02–10.84)	3.77 (0.1–11.01)	4.99 (0.59–10.87)	4.34 (1.19–9.58)	5.29 (0–12.81)	6.19 (0.04–12.83)	0.043*
Heart-V_{10} Gy [%]	1.28 (0–7.91)	2.01 (0–7.59)	2.71 (0.01–7.73)	2.24 (0.12–68.14)	3.09 (0–8.24)	3.17 (0–8.54)	NS
Heart-V_{17} Gy [%]	0.76 (0–6.61)	1.22 (0–6.08)	2.03 (0–6.52)	1.36 (0–4.79)	2.37 (0–6.92)	3.36 (0–6.42)	NS
Heart-V_{20} Gy [%]	0.62 (0–6.22)	1 (0–5.63)	1.83 (0–6.16)	1.17 (0–4.38)	2.15 (0–6.51)	2.01 (0–5.81)	NS
Heart-V_{35} Gy [%]	0.15 (0–4.12)	0.2 (0–3.4)	0.93 (0–4.15)	0.31 (0–2.3)	1.06 (0–4.32)	0.63 (0–2.91)	NS
Heart-V_{40} Gy [%]	0.02 (0–1.41)	0.01 (0–1.65)	0.24 (0–1.45)	0.03 (0–0.42)	0.03 (0–1.93)	0.04 (0–1.69)	NS
LV-D_{mean} [Gy]	2.3 (0.7–5.7)	2.9 (1.31–5.84)	3.2 (1.1–6.9)	3.15 (1.78–5.97)	3.5 (1.3–8.0)	3.92 (1.83–7.25)	0.019*
LV-V_5 Gy [%]	6.8 (0–17.4)	8.27 (0–17.39)	9.7 (0–22.0)	8.47 (0.46–19.87)	10.8 (0–26.3)	12 (0–26.02)	0.052*
LV-V_{23} Gy [%]	1.4 (0–9.5)	1.73 (0–8.47)	2.8 (0–12.0)	1.81 (0–8.18)	3.3 (0–14.3)	3.1 (0–10.58)	NS
LV anterior-D_{mean} [Gy]	3.6 (1.2–12.8)	4.86 (1.94–12.35)	6.8 (2.0–15.9)	5.71 (2.69–14.48)	6.8 (1.9–20.1)	6.94 (2.58–19.18)	0.017*
LV lateral-D_{mean} [Gy]	1.6 (0.7–2.8)	2.16 (1.18–3.38)	1.8 (0.9–6.3)	2.24 (1.55–5.12)	2.5 (1.2–8.7)	2.98 (1.73–7.59)	< 0.001*, < 0.001†
LV inferior-D_{mean} [Gy]	0.5 (0.3–3.3)	0.96 (0.77–1.17)	0.6 (0.5–0.9)	1.07 (0.9–1.32)	0.8 (0.6–2.0)	1.33 (0.96–1.98)	< 0.005*, < 0.005†
LV septal-D_{mean} [Gy]	1.2 (0.4–3.4)	1.8 (1.01–3.71)	1.6 (1.1–3.4)	2.19 (1.77–3.74)	1.9 (1.2–3.9)	2.56 (1.72–4.46)	< 0.005*, < 0.005†
LV apical-D_{mean} [Gy]	6.9 (1.2–19.6)	8.54 (1.64–19.79)	9.0 (1.7–21.9)	8.42 (2.46–19.68)	9.5 (1.2–24.8)	8.91 (1.76–22.16)	NS
LADCA-D_{mean} [Gy]	5.2 (1.2–27.9)	6.84 (1.8–27.62)	13.8 (2.6–25.2)	10.76 (3.01–20.73)	11.1 (2.2–21.2)	8.24 (2.84–21.22)	NS
LADCA-V_{30} Gy [%]	0.2 (0–66.3)	0.36 (0–63.48)	17.8 (0–59.0)	7.39 (0–84.2)	8.9 (0–43.3)	2.13 (0–46.34)	NS
LADCA-V_{40} Gy [%]	0 (0–37.8)	0 (0–43.09)	0.5 (0–32.9)	0 (0–3.22)	0 (0–19.2)	0 (0–7.26)	NS
LADCA-prox-D_{mean} [Gy]	1.6 (0.6–8.6)	2.22 (1.22–7.95)	2.9 (0.6–7.2)	2.96 (1.96–5.19)	2.5 (1.4–7.2)	2.84 (2.07–12.43)	< 0.001*, 0.002†
LADCA-mid-D_{mean} [Gy]	7.9 (1.6–40.0)	9.12 (2.26–39.63)	17.9 (2.0–38.7)	13.81 (4.22–30.95)	10.4 (2.5–29.8)	11.14 (3.23–36.01)	NS
LADCA-dist-D_{mean} [Gy]	5.5 (1.4–41.1)	8.58 (2.03–40.65)	26.9 (3.5–39.4)	17.46 (3.98–35.39)	14.0 (2.4–39.7)	16.32 (2.87–34.95)	NS

*intergroup comparison within 3D-CRT technique, using Kruskal-Wallis test; † intergroup comparison within t-IMRT technique using Kruskal-Wallis test; 3D-CRT = three-dimensional conformal radiotherapy; CTV = clinical target volume; D_{mean} = mean dose; dist = distal; Gy = Gray; LADCA = left anterior descending artery; LV = left ventricle; mid = middle; MWHD = whole heart mean dose; NS = not significant; prox = proximal; t-IMRT = tangential intensity modulated radiation therapy; V_x Gy = fractional volume receiving x Gy

Despite the low MWHD for the whole group, our study confirms that apical and anterior parts of LV and mid or distal LADCA segments in both 3D-CRT and t-IMRT techniques receive disproportionately higher D_{mean} radiation doses. Likewise, in the study by Tang *et al*., segments corresponding to anterior and apical LV wall absorbed the highest doses, 9.2 Gy and 14.9 Gy, respectively. Patients were treated with tangential breast RT, with or without regional nodal irradiation and with or without DIBH.[36] Corresponding values in our study were lower in both evaluated techniques, 3D-CRT *vs.* t-IMRT for anterior and apical LV walls were 5.0 *vs.* 5.4 Gy and 8.5 *vs.* 8.9 Gy, respectively. Lower numbers might reflect a difference in contoured thickness of the LV wall, 6-9 mm in the study of Tang *et al.* compared to 10 mm used in our study, as suggested by Duane *et al.*[24]

In our work, the LADCA-D_{mean} was 8.2 Gy (range, 1.2–27.9) in 3D-CRT and 8.4 Gy (range, 1.8–27.6) in t-IMRT, respectively. Drost *et al.* in their systematic review of heart doses reported varying dose-volume measurements for the LADCA. The LADCA-D_{mean} ranged from 1.9–40.8 Gy (average 12.4 Gy)[6], which is similar to our data. In our series of treatment plans, we have demonstrated the highest D_{mean} for the middle LADCA segment in the group of women with medium-sized CTVs (17.9 Gy) but was not significantly different compared to the smallest or the largest CTV groups. With t-IMRT, it was possible to lower LADCA high-dose areas (V_{30} Gy), but not low-dose areas or mean doses to the coronary arteries. Carosi *et al.* observed no difference in MWHD when t-IMRT was compared to 3D-CRT (2.0 *vs.* 1.9 Gy) in 24 patients with a median breast volume of 645 cm^3.

However, the authors showed a statistically meaningful difference in LADCA D_{mean} (10.3 *vs.* 11.9 Gy, p=0.0003), LADCA-D_{max} and LADCA-V_{17} Gy parameters using t-IMRT compared to 3D-CRT.[48]

There are many possible explanations for the dissimilar reported heart and heart substructures' absorbed doses in free-breathing left-breast only RT. The differences may arise from the discrepancy in the total dose prescription and the size of the radiation field, CTV definition and size, OAR contouring, including diameter of the coronary arteries and LV thickness, the lack of detailed heart contouring atlases, individual coronary topology, heart size, body mass index, CWS distance, and finally radiotherapy technique used.[9,33,49–52] The use of contrast agent[53] or automatic substructures' segmentation without[54] or with cardiac magnetic resonance imaging[55] could improve contouring consistency, but these technical solutions are unlikely to be widely adopted in the near future. Non-automatic contouring is feasible as showed in a study by Francolini *et al.* Authors made multiple comparisons of delineated cardiac chambers and 5 left LV wall segments according to aforementioned cardiac atlas[24] and confirmed high interobserver delineation consistency.[56]

Spatial variation in contouring has been shown to result in less than 1 Gy dose variation for most segments and in most regimens in adjuvant breast cancer RT, but higher dose variations up to 21.8 Gy were seen for segments close to the radiation field edge.[24] Substantial variation in the estimated dose was observed for LADCA, regardless of which particular delineation guidelines were used.[57] Except for proximal LADCA (2.6 Gy *vs.* 2.5 Gy), absorbed mean D_{mean} values of LADCA segments and LV were lower in our study compared to the partially wide tangential technique used in Duane and coworkers' research; 15.1 Gy *vs.* 25.1 Gy for middle LADCA segment, 17.6 Gy *vs.* 35.8 Gy for distal LADCA segment, and 3.2 *vs.* 6.7 Gy for LV. In the study of Wennstig *et al.*, three radiation oncologists, using the heart atlas of Feng *et al.*, achieved substantial spatial agreement in delineating coronary arteries on 32 CT study sets. The agreement was the highest for LMCA and LADCA, and less for RCA.[23,58] In our study, the coronary vessel diameter was set to 6 mm considering both cardiac and respiratory motion, similar to Wennstig and colleagues' work.[23]

Based on recent clinical reports, the DEGRO group proposed stringent dose constraints for the heart and its substructures in adjuvant breast cancer radiation treatment.[42] We surpassed at least one of the proposed optimal dose constraints for LV (D_{mean} < 3 Gy, V_5 < 17%, and V_{23} < 5%) or LADCA (D_{mean} < 10 Gy, V_{30} < 2%, and V_{40} < 1%) in 11.7–51.7% of all evaluated plans. In our plan optimization process, we did not use specific dose-volume constraints for cardiac substructures. However, it has been shown that additional LADCA or LV constraints in breast cancer adjuvant 3D-CRT or IMRT treatment planning might help to optimize heart dosimetric metrics further.[23,59]

In our study, the evaluation of the planned dose to the heart and specific cardiac substructures was performed in a free-breathing simulation CT scan and in the supine position. Ideally, the dose to cardiac substructures should also be evaluated for patients treated using alternative treatment positions (lateral decubitus or prone) or with DIBH. Due to various reasons, most patients are still treated in the conventional free-breathing supine position, whereas prone positioning or DIBH is in the best-case scenario offered to only 28–83% of breast cancer patients.[15,60] All delineations were performed on a non-enhanced CT scan, an approach that may impact the visibility of the small cardiac segments. Additional drawback of our study is not including patients receiving peri-clavicular regional nodal irradiation with or without internal mammary lymph chain irradiation. Strengths of this study include careful contouring of individual cardiac substructures and using a cardiac atlas based on individual anatomy. An experienced cardiac radiologist thoroughly evaluated the contours.

Conclusions

This is the first study to evaluate the cardiac contouring atlas for radiotherapy by Duane *et al.*[24] simultaneously considering different CTV size. We confirmed that regardless of very low D_{mean} values for the whole heart achieved using a 3D-CRT or t-IMRT free-breathing adjuvant RT technique for breast cancer, a small volume of the heart may receive disproportionate D_{mean} or D_{max} values exceeding 40 Gy. We observed differences in heart dosimetric metrics between the small, medium, and large CTV sizes for both evaluated techniques, which may disappear with DIBH technique. With t-IMRT technique, only few dosimetric metrics were improved compared to 3D-CRT. The observed results in our study suggest that anatomic differences, especially breast volume and CWS, should be considered in clinical practice as well as in the dosimetric studies of various treatment plan-

ning techniques. Subdividing breast target volume into similar cohorts could be helpful in this context and further research is warranted. The quantification of the radiation dose variability of individual cardiac substructures is an important first step to understand the unique cardiac structures' dose-volume predictors for cardiotoxicity in adjuvant, free-breathing breast cancer radiation therapy. In the future, reported absorbed doses may be paired with cardiac imaging and help to choose patients for whom more intense cardiac function monitoring is warranted.

References

1. Abdel-Qadir H, Austin PC, Lee DS, Amir E, Tu J V, Thavendiranathan P, et al. A population-based study of cardiovascular mortality following early-stage breast cancer. *JAMA Cardiol* 2017; **2:** 88. doi: 10.1001/jamacardio.2016.3841
2. Weberpals J, Jansen L, Müller OJ, Brenner H. Long-term heart-specific mortality among 347 476 breast cancer patients treated with radiotherapy or chemotherapy: a registry-based cohort study. *Eur Heart J* 2018; **39:** 3896-903. doi: 10.1093/eurheartj/ehy167
3. Darby SC, Ewertz M, Hall P. Ischemic heart disease after breast cancer radiotherapy. N *Engl J Med* 2013; **368:** 2527. doi: 10.1056/NEJMc1304601
4. van den Bogaard VAB, Ta BDP, van der Schaaf A, Bouma AB, Middag AMH, Bantema-Joppe EJ, et al. Validation and modification of a prediction model for acute cardiac events in patients with breast cancer treated with radiotherapy based on three-dimensional dose distributions to cardiac substructures. *J Clin Oncol* 2017; **35:** 1171-8; doi: 10.1200/JCO.2016.69.8480
5. Saiki H, Petersen IA, Scott CG, Bailey KR, Dunlay SM, Finley RR, et al. Risk of heart failure with preserved ejection fraction in older women after contemporary radiotherapy for breast cancer. *Circulation* 2017; **135:** 1388-96. doi: 10.1161/CIRCULATIONAHA.116.025434
6. Drost L, Yee C, Lam H, Zhang L, Wronski M, McCann C, et al. A systematic review of heart dose in breast radiotherapy. *Clin Breast Cancer* 2018; **18:** e819-24. doi: 10.1016/j.clbc.2018.05.010
7. Taylor CW, Wang Z, Macaulay E, Jagsi R, Duane F, Darby SC. Exposure of the heart in breast cancer radiation therapy: a systematic review of heart doses published during 2003 to 2013. *Int J Radiat Oncol Biol Phys* 2015; **93:** 845-53. doi: 10.1016/j.ijrobp.2015.07.2292
8. Taylor C, Correa C, Duane FK, Aznar MC, Anderson SJ, Bergh J, et al. Estimating the risks of breast cancer radiotherapy: evidence from modern radiation doses to the lungs and heart and from previous randomized trials. *J Clin Oncol* 2017; **35:** 1641-9. doi: 10.1200/JCO.2016.72.0722
9. Pierce LJ, Feng M, Griffith KA, Jagsi R, Boike T, Dryden D, et al. Recent time trends and predictors of heart dose from breast radiation therapy in a large quality consortium of radiation oncology practices. *Int J Radiat Oncol* 2017; **99:** 1154-61. doi: 10.1016/j.ijrobp.2017.07.022
10. Jacobse JN, Duane FK, Boekel NB, Schaapveld M, Hauptmann M, Hooning MJ, et al. Radiation dose-response for risk of myocardial infarction in breast cancer survivors. *Int J Radiat Oncol Biol Phys* 2018; **103:** 595-604. doi: 10.1016/j.ijrobp.2018.10.025
11. Karpf D, Sakka M, Metzger M, Grabenbauer GG. Left breast irradiation with tangential intensity modulated radiotherapy (t-IMRT) versus tangential volumetric modulated arc therapy (t-VMAT): trade-offs between secondary cancer induction risk and optimal target coverage. *Radiat Oncol* 2019; **14:** 156. doi: 10.1186/s13014-019-1363-4
12. Halasz LM, Patel SA, McDougall JA, Fedorenko C, Sun Q, Goulart BHL, et al. Intensity modulated radiation therapy following lumpectomy in early-stage breast cancer: patterns of use and cost consequences among Medicare beneficiaries. *PLoS One* 2019; **14:** e0222904. doi: 10.1371/journal.pone.0222904
13. Jin G, Chen LX, Deng XW, Liu XW, Huang Y, Huang XB. A comparative dosimetric study for treating left-sided breast cancer for small breast size using five different radiotherapy techniques: conventional tangential field; filed-in-filed; tangential-IMRT; multi-beam IMRT and VMAT. *Radiat Oncol* 2013; **8:** 89. doi: 10.1186/1748-717X-8-89
14. Lee G, Rosewall T, Fyles A, Harnett N, Dinniwell RE. Anatomic features of interest in women at risk of cardiac exposure from whole breast radiotherapy. *Radiother Oncol* 2015; **115:** 355-60. doi: 10.1016/j.radonc.2015.05.002
15. Desai N, Currey A, Kelly T, Bergom C. Nationwide trends in heart-sparing techniques utilized in radiation therapy for breast cancer. *Adv Radiat Oncol* 2019; **4:** 246-52. doi: 10.1016/j.adro.2019.01.001
16. Mendez LC, Louie A V., Moreno C, Wronski M, Warner A, Leung E, et al. Evaluation of a new predictor of heart and left anterior descending artery dose in patients treated with adjuvant radiotherapy to the left breast. *Radiat Oncol* 2018; **13:** 124. doi: 10.1186/s13014-018-1069-z
17. Guan H, Dong Y-L, Ding L-J, Zhang Z-C, Huang W, Liu C-X, et al. Morphological factors and cardiac doses in whole breast radiation for left-sided breast cancer. *Asian Pac J Cancer Prev* 2015; **16:** 2889-94. doi: 10.7314/apjcp.2015.16.7.2889
18. Hannan R, Thompson RF, Chen Y, Bernstein K, Kabarriti R, Skinner W, et al. Hypofractionated whole-breast radiation therapy: does breast size matter? *Int J Radiat Oncol* 2012; **84:** 894-901. doi: 10.1016/j.ijrobp.2012.01.093
19. Yang DS, Lee JA, Yoon WS, et al. Whole breast irradiation for small-sized breasts after conserving surgery: is the field-in-field technique optimal? *Breast Cancer* 2014; **21:** 162-9. doi: 10.1007/s12282-012-0365-y
20. Vicini FA, Sharpe M, Kestin L, Martinez A, Mitchell CK, Wallace MF, et al. Optimizing breast cancer treatment efficacy with intensity-modulated radiotherapy. *Int J Radiat Oncol Biol Phys* 2002; **54:** 1336-44. doi: 10.1016/S0360-3016(02)03746-X
21. Michalski A, Atyeo J, Cox J, Rinks M, Morgia M, Lamoury G. A dosimetric comparison of 3D-CRT, IMRT, and static tomotherapy with an SIB for large and small breast volumes. *Med Dosim* 2014; **39:** 163-8. doi: 10.1016/j.meddos.2013.12.003
22. Ratosa I, Jenko A, Oblak I. Breast size impact on adjuvant radiotherapy adverse effects and dose parameters in treatment planning. *Radiol Oncol* 2018; **52:** 233-44. doi: 10.2478/raon-2018-0026
23. Wennstig A-K, Garmo H, Hållström P, Nyström PW, Edlund P, Blomqvist C, et al. Inter-observer variation in delineating the coronary arteries as organs at risk. *Radiother Oncol* 2017; **122:** 72-8. doi: 10.1016/j.radonc.2016.11.007
24. Duane F, Aznar MC, Bartlett F, Cutter DJ, Darby SC, Jagsi R, et al. A cardiac contouring atlas for radiotherapy. *Radiother Oncol* 2017; **122:** 416-22. doi: 10.1016/j.radonc.2017.01.008
25. Skyttä T, Tuohinen S, Boman E, Virtanen V, Raatikainen P, Kellokumpu-Lehtinen P-L. Troponin T-release associates with cardiac radiation doses during adjuvant left-sided breast cancer radiotherapy. *Radiat Oncol* 2015; **10:** 141. doi: 10.1186/s13014-015-0436-2
26. D'Errico MP, Petruzzelli MF, Gianicolo EAL, Grimaldi L, Loliva F, Tramacere F, et al. Kinetics of B-type natriuretic peptide plasma levels in patients with left-sided breast cancer treated with radiation therapy: results after one-year follow-up. *Int J Radiat Biol* 2015; **91:** 804-9. doi: 10.3109/09553002.2015.1027421
27. Kaidar-Person O, Zagar TM, Oldan JD, Matney J, Jones EL, Das S, et al. Early cardiac perfusion defects after left-sided radiation therapy for breast cancer: is there a volume response? *Breast Cancer Res Treat* 2017; **164:** 253-62. doi: 10.1007/s10549-017-4248-y
28. Lind PA, Pagnanelli R, Marks LB, Borges-Neto S, Hu C, Zhou SM, et al. Myocardial perfusion changes in patients irradiated for left-sided breast cancer and correlation with coronary artery distribution. *Int J Radiat Oncol Biol Phys* 2003; **55:** 914-20. doi: 10.1016/s0360-3016(02)04156-1
29. Zyromska A, Malkowski B, Wisniewski T, Majewska K, Reszke J, Makarewicz R. (15)O-H2O PET/CT as a tool for the quantitative assessment of early post-radiotherapy changes of heart perfusion in breast carcinoma patients. *Br J Radiol* 2018; **91:** 20170653. doi: 10.1259/bjr.20170653
30. Tuohinen SS, Skyttä T, Virtanen V, Virtanen M, Luukkaala T, Kellokumpu-Lehtinen P-L, et al. Detection of radiotherapy-induced myocardial changes by ultrasound tissue characterisation in patients with breast cancer. *Int J Cardiovasc Imaging* 2016; **32:** 767-76. doi: 10.1007/s10554-016-0837-9

31. Heggemann F, Grotz H, Welzel G, Dösch C, Hansmann J, Kraus-Tiefenbacher U, et al. Cardiac function after multimodal breast cancer therapy assessed with functional magnetic resonance imaging and echocardiography imaging. *Int J Radiat Oncol Biol Phys* 2015; **93:** 836-44. doi: 10.1016/j.ijrobp.2015.07.2287

32. Erven K, Florian A, Slagmolen P, Sweldens C, Jurcut R, Wildiers H, et al. Subclinical cardiotoxicity detected by strain rate imaging up to 14 months after breast radiation therapy. *Int J Radiat Oncol* 2013; **85:** 1172-8. doi: 10.1016/j.ijrobp.2012.09.022

33. Jacob S, Camilleri J, Derreumaux S, Walker V, Lairez O, Lapeyre M, et al. Is mean heart dose a relevant surrogate parameter of left ventricle and coronary arteries exposure during breast cancer radiotherapy: a dosimetric evaluation based on individually-determined radiation dose (BACCARAT study). *Radiat Oncol* 2019; **14:** 29. doi: 10.1186/s13014-019-1234-z

34. Duma MN, Herr A-C, Borm KJ, Trott KR, Molls M, Oechsner M, et al. Tangential field radiotherapy for breast cancer—the dose to the heart and heart subvolumes: what structures must be contoured in future clinical trials? *Front Oncol* 2017; **7:** 130. doi: 10.3389/fonc.2017.00130

35. Becker-Schiebe M, Stockhammer M, Hoffmann W, Wetzel F, Franz H. Does mean heart dose sufficiently reflect coronary artery exposure in left-sided breast cancer radiotherapy? *Strahlenther Onkol* 2016; **192:** 624-31. doi: 10.1007/s00066-016-1011-y

36. Tang S, Otton J, Holloway L, Delaney GP, Liney G, George A, et al. Quantification of cardiac subvolume dosimetry using a 17 segment model of the left ventricle in breast cancer patients receiving tangential beam radiotherapy. *Radiother Oncol* 2019; **132:** 257-65. doi: 10.1016/j.radonc.2018.09.021

37. Tong Y, Yin Y, Cheng P, Lu J, Liu T, Chen J, et al. Quantification of variation in dose–volume parameters for the heart, pericardium and left ventricular myocardium during thoracic tumor radiotherapy. *J Radiat Res* 2018; **59:** 462-8. doi: 10.1093/jrr/rry026

38. Taylor C, McGale P, Brønnum D, Correa C, Cutter D, Duane FK, et al. Cardiac structure injury after radiotherapy for breast cancer: cross-sectional study with individual patient data. *J Clin Oncol* 2018; **36:** 2288-96. doi: 10.1200/JCO.2017.77.6351

39. Abouegylah M, Braunstein LZ, Alm El-Din MA, Niemierko A, Salama L, Elebrashi M, et al. Evaluation of radiation-induced cardiac toxicity in breast cancer patients treated with Trastuzumab-based chemotherapy. *Breast Cancer Res Treat* 2018; **174:** 179-85. doi: 10.1007/s10549-018-5053-y

40. Moignier A, Broggio D, Derreumaux S, Beaudré A, Girinsky T, Paul J-F, et al. Coronary stenosis risk analysis following Hodgkin lymphoma radiotherapy: a study based on patient specific artery segments dose calculation. *Radiother Oncol* 2015; **117:** 467-72. doi: 10.1016/j.radonc.2015.07.043

41. Jacobse JN, Duane FK, Boekel NB, Schaapveld M, Hauptmann M, Hooning MJ, et al. Radiation dose-response for risk of myocardial infarction in breast cancer survivors. *Int J Radiat Oncol Biol Phys* 2019; **103:** 595-604. doi: 10.1016/j.ijrobp.2018.10.025

42. Piroth MD, Baumann R, Budach W, Dunst J, Feyer P, Fietkau R, et al. Heart toxicity from breast cancer radiotherapy. *Strahlenther Onkol* 2019; **195:** 1-12. doi: 10.1007/s00066-018-1378-z

43. Lang RM, Badano LP, Mor-Avi V, Afilalo J, Armstrong A, Ernande L, et al. Recommendations for cardiac chamber quantification by echocardiography in adults: an update from the American Society of Echocardiography and the European Association of Cardiovascular Imaging. *J Am Soc Echocardiogr* 2015; **28:** 1-39.e14. doi: 10.1016/j.echo.2014.10.003

44. Cerqueira MD, Weissman NJ, Dilsizian V, Jacobs AK, Kaul S, Laskey WK, et al. Standardized myocardial segmentation and nomenclature for tomographic imaging of the heart. A statement for healthcare professionals from the Cardiac Imaging Committee of the Council on Clinical Cardiology of the American Heart Association. *Circulation* 2002; **105:** 539-42. doi: 10.1161/hc0402.102975

45. Offersen B V., Boersma LJ, Kirkove C, Hol S, Aznar MC, Sola AB, et al. ESTRO consensus guideline on target volume delineation for elective radiation therapy of early stage breast cancer, version 1.1. *Radiother Oncol* 2015; **114:** 3-10. doi: 10.1016/j.radonc.2014.11.030

46. De Rose F, Fogliata A, Franceschini D, Iftode C, Torrisi R, Masci G, et al. Hypofractionated volumetric modulated arc therapy in ductal carcinoma in situ: toxicity and cosmetic outcome from a prospective series. *Br J Radiol* 2018; **91:** 20170634. doi: 10.1259/bjr.20170634

47. Fogliata A, De Rose F, Franceschini D, Stravato A, Seppälä J, Scorsetti M, et al. Critical appraisal of the risk of secondary cancer induction from breast radiation therapy with volumetric modulated arc therapy relative to 3D conformal therapy. *Int J Radiat Oncol Biol Phys* 2018; **100:** 785-93. doi: 10.1016/j.ijrobp.2017.10.040

48. Carosi A, Ingrosso G, Turturici I, Valeri S, Barbarino R, Di Murro L, et al. Whole breast external beam radiotherapy in elderly patients affected by left-sided early breast cancer: a dosimetric comparison between two simple free-breathing techniques. *Aging Clin Exp Res* 2020; **32:** 1335-41. doi: 10.1007/s40520-019-01312-5

49. Moignier A, Broggio D, Derreumaux S, El Baf F, Mandin A-M, Girinsky T, et al. Dependence of coronary 3-dimensional dose maps on coronary topologies and beam set in breast radiation therapy: a study based on CT angiographies. *Int J Radiat Oncol Biol Phys* 2014; **89:** 182-90. doi: 10.1016/j.ijrobp.2014.01.055

50. Mkanna A, Mohamad O, Ramia P, Thebian R, Makki M, Tamim H, et al. Predictors of cardiac sparing in deep inspiration breath-hold for patients with left sided breast cancer. *Front Oncol* 2018; **8:** 564. doi: 10.3389/fonc.2018.00564

51. Wollschläger D, Karle H, Stockinger M, Bartkowiak D, Bührdel S, Merzenich H, et al. Radiation dose distribution in functional heart regions from tangential breast cancer radiotherapy. *Radiother Oncol* 2016; **119:** 65-70. doi: 10.1016/j.radonc.2016.01.020

52. Appelt AL, Vogelius IR, Bentzen SM. Modern hypofractionation schedules for tangential whole breast irradiation decrease the fraction size-corrected dose to the heart. *Clin Oncol (R Coll Radiol)* 2013; **25:** 147-52. doi: 10.1016/j.clon.2012.07.012

53. Lee J, Hua K-L, Hsu S-M, Lin J-B, Lee C-H, Lu K-W, et al. Development of delineation for the left anterior descending coronary artery region in left breast cancer radiotherapy: an optimized organ at risk. *Radiother Oncol* 2017; **122:** 423-30. doi: 10.1016/j.radonc.2016.12.029

54. Van Dijk-Peters FBJ, Sijtsema NM, Kierkels RGJ, Vliegenthart R, Langendijk JA, Maduro JH, et al. OC-0259: validation of a multi-atlas based auto-segmentation of the heart in breast cancer patients. *Radiother Oncol* 2015; **115:** S132-3. doi: 10.1016/S0167-8140(15)40257-9

55. Morris ED, Ghanem AI, Pantelic M V, Walker EM, Han X, Glide-Hurst CK. Cardiac substructure segmentation and dosimetry using a novel hybrid MR/CT cardiac atlas. *Int J Radiat Oncol Biol Phys* 2018; **103:** 985-93; doi: 10.1016/j.ijrobp.2018.11.025

56. Francolini G, Desideri I, Meattini I, Becherini C, Terziani F, Olmetto E, et al. Assessment of a guideline-based heart substructures delineation in left-sided breast cancer patients undergoing adjuvant radiotherapy: quality assessment within a randomized phase III trial testing a cardioprotective treatment strategy (SAFE-2014). *Strahlenther Onkol* 2019; **195:** 43-51. doi: 10.1007/s00066-018-1388-x

57. Lorenzen EL, Taylor CW, Maraldo M, Nielsen MH, Offersen B V, Andersen MR, et al. Inter-observer variation in delineation of the heart and left anterior descending coronary artery in radiotherapy for breast cancer: a multi-centre study from Denmark and the UK. *Radiother Oncol* 2013; **108:** 254-8. doi: 10.1016/j.radonc.2013.06.025

58. Feng M, Moran JM, Koelling T, Chughtai A, Chan JL, Freedman L, et al. Development and validation of a heart atlas to study cardiac exposure to radiation following treatment for breast cancer. *Int J Radiat Oncol Biol Phys* 2011; **79:** 10-8. doi: 10.1016/j.ijrobp.2009.10.058

59. Tan W, Wang X, Qiu D, Liu D, Jia S, Zeng F, et al. Dosimetric comparison of intensity-modulated radiotherapy plans, with or without anterior myocardial territory and left ventricle as organs at risk, in early-stage left-sided breast cancer patients. *Int J Radiat Oncol Biol Phys* 2011; **81:** 1544-51. doi: 10.1016/j.ijrobp.2010.09.028

60. Park HJ, Oh DH, Shin KH, Kim JH, Choi DH, Park W, et al. Patterns of practice in radiotherapy for breast cancer in Korea. *J Breast Cancer* 2018; **21:** 244-50. doi: 10.4048/jbc.2018.21.e37